PIER C

(Received 3 July 2024, Accepted 19 August 2024, Scheduled 8 September 2024)

A Planar Five-Section Short-Length Coupled-Line Band-Stop Filter with Two Reconfigured States

Mengxin He[1,2], Xiaoying Zuo[1,2,*], Hang Mei[1,2], and Yajian Li[1,2]

[1] *Beijing Key Laboratory for Sensor, Beijing Information Science & Technology University, Beijing 100192, China*
[2] *School of Applied Science, Beijing Information Science & Technology University, Beijing 100192, China*

ABSTRACT: A novel circuit structure is proposed to design a small size band-stop filter (BSF). The structure consists of five pairs of short coupled-lines. The bandwidth, roll off and center frequency of the filter can be flexibly controlled by changing the data of different pairs of coupled-lines. By disconnecting the left-most pair of coupled-lines, the band-stop filter can be transformed into a full resistance filter. The center frequency of the band-stop filter is 2.40 GHz. The measured 20-dB stopband insertion loss bandwidth is 29.2% (2.05–2.75 GHz, the highest measured rejection is 44.21 dB). The simulation results agree well with the measured ones, which verifies the effectiveness of the proposed structure. The use of coupled-lines makes the structure more compact. The circuit size is $0.35\lambda_g \times 0.27\lambda_g$ ($25.63\,\text{mm} \times 19.70\,\text{mm}$).

1. INTRODUCTION

Band-stop filters are widely used in wireless communication systems. With the development of science and technology, band-stop filters with controllable bandwidth, different configuration states, and compact size have become a demand. Based on the amount of signal that can be blocked, filters can be divided into single-band [1], dual-band [2], and multi-band [3] band-stop filters. Traditionally, a band-stop filter is designed by inserting an open/short circuit resonator between the transmission lines [4]. However, the size of the filter can be effectively reduced by using coupled-lines [5]. To achieve miniaturization, two open stubs and an open complementary split ring resonator are employed [6], with the open stubs folded in the opposite direction. By folding the dominant area around the main structure [7], significant miniaturization is achieved.

Increasing the number of transmission zeros (TZs) can better control the bandwidth. In [8], four TZs are generated to manipulate the bandwidth by the source-load coupling. According to [9], a band-stop filter consisting of two pairs of coupled-lines is proposed, and the influence of each pair of coupled-lines on TZs and stopband bandwidth is analyzed. However, the TZs of filters with more coupled-lines are rarely mentioned.

In order to achieve tunability, a compact reconfigurable filter is proposed [10], which adopts a resonant element in the form of a folded slot. By placing a positive-intrinsic-negative (PIN) diode in the center of slot, the filter can be configured to band-stop and all-pass states [11]. [12] switches between multifrequency band-pass filter and band-stop filter modes by changing the coupling path between source and load. [13] presents an RF input-quasi-reflectionless band-pass filter with reconfigurable center frequency by tuning range through the novel technique.

In this paper, a compact band-stop filter with five pairs of short coupled-lines is proposed. The first and second pairs of coupled-lines mainly affect S_{11}, and the remaining three pairs of coupled-lines can control S_{21} and adjust the bandwidth. For demonstration, a band-stop filter is implemented and measured. The stopband 20-dB insertion loss bandwidth measured by the filter at the center frequency is 700 MHz (2.05 GHz–2.75 GHz), and the circuit size is $25.63\,\text{mm} \times 19.70\,\text{mm}$ ($0.35 \times 0.27\lambda_g^2$ where λ_g is the guided wavelength at the center frequency). Moreover, by changing the connection state of the first pair of coupled-lines, the filter can switch between band-stop and full-resistance states.

2. ANALYSIS AND DESIGN

The circuit configuration of the proposed band-stop filter is shown in Fig. 1 (Structure I). The left structure of the filter is composed of two pairs of coupled-lines, and the right part is composed of three pairs of coupled-lines. By disconnecting the left-most pair of coupled-lines, the band-stop filter can be transformed into a full resistance filter (Structure II). The even-mode and odd-mode impedance (Z_{ei}, Z_{oi}, $i = 1, 2, 3, 4, 5$) and electrical length (θ) of the five coupled-lines are also defined in Fig. 1.

Since the proposed structure is symmetric, even- and odd-mode analysis can be performed. The odd-mode and even-mode equivalent circuit of bandstop filter is shown in Fig. 2. Z_{ino} and Z_{ine} respectively represent the input impedance under parity excitation.

2.1. Structure Analysis

Based on odd-mode equivalent circuits, Z_{ino1}, Z_{ino2}, Z_{ino3}, Z_{ino4}, and Z_{ino5} are the input impedances. They are calculated

* Corresponding author: Xiaoying Zuo (zuoxiaoying03@163.com).

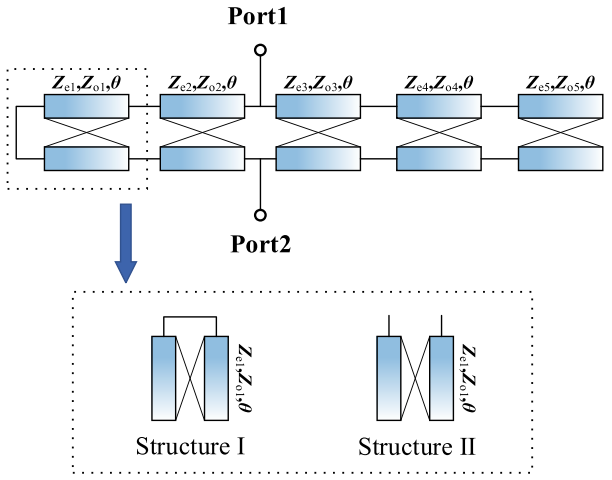

FIGURE 1. The circuit configuration of the proposed filter.

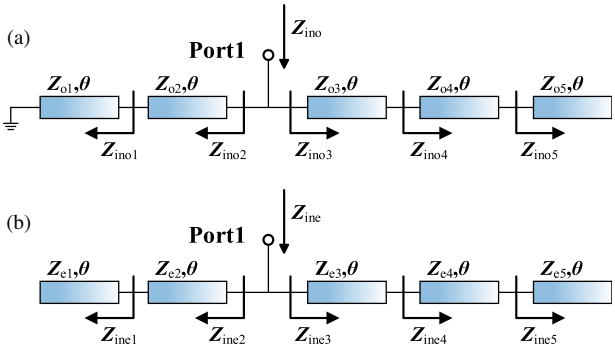

FIGURE 2. The (a) odd-mode and (b) even-mode equivalent circuits of the proposed bandstop filter.

as

$$\begin{cases} Z_{ino1} = jZ_{o1}\tan\theta \\ Z_{ino2} = j\,\frac{Z_{o2}^2\tan\theta + Z_{o1}Z_{o2}\tan\theta}{-Z_{o1}\tan^2\theta + Z_{o2}} \\ Z_{ino3} = Z_{o3}\,\frac{Z_{ino4}+jZ_{o3}\tan\theta}{Z_{o3}+jZ_{ino4}\tan\theta} \\ Z_{ino4} = j\,\frac{Z_{o4}^2\tan^2\theta - Z_{o4}Z_{o5}}{(Z_{o4}+Z_{o5})\tan\theta} \\ Z_{ino5} = -jZ_{o5}\cot\theta \end{cases} \tag{1}$$

Similar to odd-mode analysis, Z_{ine1}, Z_{ine2}, Z_{ine3}, Z_{ine4}, and Z_{ine5} are

$$\begin{cases} Z_{ine1} = -jZ_{e1}\cot\theta \\ Z_{ine2} = j\,\frac{Z_{e2}^2\tan^2\theta - Z_{e1}Z_{e2}}{(Z_{e1}+Z_{e2})\tan\theta} \\ Z_{ine3} = Z_{e3}\,\frac{Z_{ine4}+jZ_{e3}\tan\theta}{Z_{e3}+jZ_{ine4}\tan\theta} \\ Z_{ine4} = j\,\frac{Z_{e4}^2\tan^2\theta - Z_{e4}Z_{e5}}{(Z_{e4}+Z_{e5})\tan\theta} \\ Z_{ine5} = -jZ_{e5}\cot\theta \end{cases} \tag{2}$$

According to transmission line theory

$$\begin{cases} Z_{ine} = \frac{Z_{ine2}Z_{ine3}}{Z_{ine2}+Z_{ine3}} \\ Z_{ino} = \frac{Z_{ino2}Z_{ino3}}{Z_{ino2}+Z_{ino3}} \end{cases} \tag{3}$$

Then the S-parameters are as follows:

$$\begin{cases} S_{11} = S_{22} = \frac{Z_0^2 - Z_{ine}Z_{ino}}{(Z_{ino}+Z_0)(Z_{ine}+Z_0)} \\ S_{12} = S_{21} = \frac{Z_0(Z_{ine}-Z_{ino})}{(Z_{ino}+Z_0)(Z_{ine}+Z_0)} \end{cases} \tag{4}$$

where Z_0 is the port impedance at ports 1 and 2.

2.2. Transmission Zeros

In formula (4), when $|S_{21}| = 0$, then $Z_{ine} = Z_{ino}$, the transmission zeros and stopband can be derived. Formula (3) can be transformed into

$$\frac{Z_{ine2}Z_{ine3}}{Z_{ine2}+Z_{ine3}} = \frac{Z_{ino2}Z_{ino3}}{Z_{ino2}+Z_{ino3}} \tag{5}$$

Based on (1)–(2), the equation for $\tan\theta$ can be calculated as:

$$A\tan^8\theta + B\tan^6\theta + C\tan^4\theta + D\tan^2\theta + E = 0 \tag{6}$$

In particular, when $Z_{ine3} = Z_{ino3}$, the equation becomes $Z_{ine2} = Z_{ino2}$, which can be finally arranged as a quadratic equation with one variable for $\tan^2\theta$.

$$\begin{aligned} &Z_{o1}Z_{e2}^2\tan^4\theta + \left(Z_{e1}Z_{o2}^2 + Z_{o1}Z_{o2}Z_{e2}\right)\tan^2\theta \\ &+Z_{e1}Z_{e2}Z_{o2} = 0 \end{aligned} \tag{7}$$

The discriminant (Δ) of quadratic formula (7) is 0, which means that $\tan^2\theta$ has two identical solutions. In the selected frequency band, there is only one transmission zero. When $\Delta < 0$, there is no internal coupling and no transmission zeros. When $\Delta > 0$, two transmission zeros are obtained. Fig. 3 shows different conditions of S_{21} with the filter with/without internal coupling.

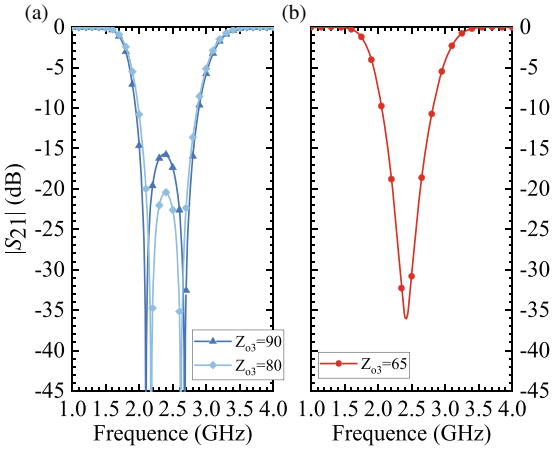

FIGURE 3. S-parameters of the BSFs (a) with/(b) without the internal coupling (Unit: Ω).

3. NUMERICAL EXAMPLES OF THE PROPOSED BAND-STOP FILTER

In order to optimize the performance of the filter, the parameters of the original design are adjusted. By generating internal coupling, not only can the filter have two transmission zeros, but also the circuit size can be reduced. The stopband width

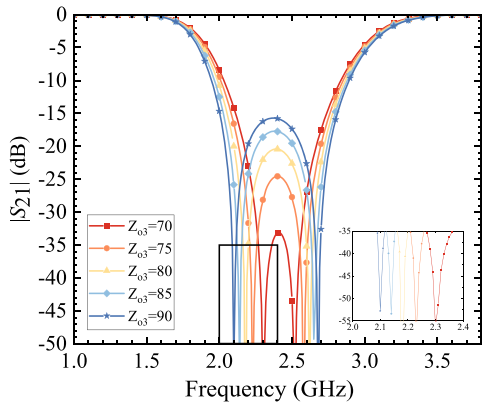

FIGURE 4. TZs positions under different values of Z_{o3} (Unit: Ω).

can be turned by setting different values for Z_{o3} as shown in Fig. 4. Changing the values of Z_{o3} from 80 to 90, as Z_{o3} increases, the stopband width becomes wider.

To get transmission poles (TPs), $|S_{11}| = 0$ is needed. Based on (1)–(2), four solutions (TP_1, TP_2, TP_3, TP_4) can be obtained in Fig. 5. As Z_{o1} decreases from 70 to 55, TP_2 and TP_3 move closer. The roll off performance is improved while maintaining 20-dB stopband suppression. The selectivity of the filter can be improved by properly adjusting Z_{o1} as shown in Fig. 5.

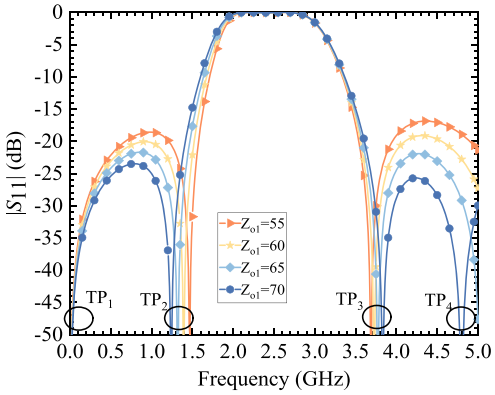

FIGURE 5. TPs positions under different values of Z_{o1} (Unit: Ω).

The electrical length (θ_5) of the right-most pair of coupled-line affects the center frequency of the bandstop filter. As shown in Fig. 6, three cases of electric length are discussed while other variables are kept invariant. As θ_5 increases from 33 to 37, the stopband frequency shifts downward, and the center frequency decreases from 2.5 GHz to 2.3 GHz. The center frequency of the band-stop filter can be adjusted by selecting a suitable θ_5.

In order to achieve the best results, the final parameters are as follows: $Z_{e1} = 75\,\Omega$, $Z_{o1} = 65\,\Omega$, $\theta_1 = 21°$, $Z_{e2} = 80\,\Omega$, $Z_{o2} = 50\,\Omega$, $\theta_2 = 20°$, $Z_{e3} = 100\,\Omega$, $Z_{o3} = 80\,\Omega$, $\theta_3 = 20°$, $Z_{e4} = 125\,\Omega$, $Z_{o4} = 75\,\Omega$, $\theta_4 = 25°$, $Z_{e5} = 90\,\Omega$, $Z_{o5} = 60\,\Omega$, $\theta_5 = 35°$.

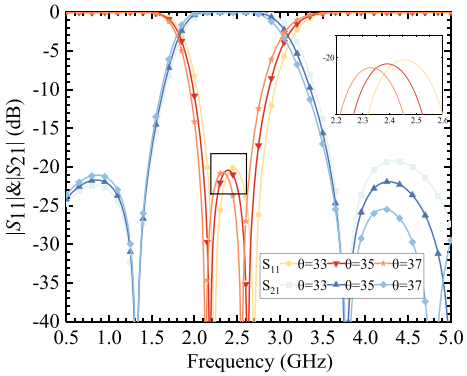

FIGURE 6. S-parameters of the BSFs with different θ_5 (Unit: °).

4. SIMULATED AND MEASURED RESULTS

To verify the proposed BSF structure, two prototype circuits were designed and fabricated on a Rogers RO4350B substrate with dielectric constant $\varepsilon_r = 3.66$, loss tangent $\tan\theta = 0.0037$, substrate thickness $h = 0.762$ mm, and 0.035 mm copper cladding. The layout and photo of the fabricated band-stop filter are shown in Fig. 7. The S-parameters of the two circuits were measured by using the vector network analyzer.

Figure 8 shows the simulated and measured results. When the center frequency of the band-stop filter is 2.40 GHz, the measured stopband 15 dB insertion loss bandwidth is 700 MHz (2.05 GHz–2.75 GHz) (the highest measured rejection is 44.21 dB). The simulated results agree well with the measured ones, which verifies the effectiveness of the proposed method. The core circuit size is $0.35\lambda_g \times 0.27\lambda_g$ (25.63 mm × 19.70 mm). Table 1 shows a comparison between this work and previous structures. The proposed PCB filter is more compact.

TABLE 1. Comparison with the state-of-the-art works.

Ref.	f_0 (GHz)	FBW	Physical dimension (mm^2)	Two Reconfigured States
[14]	3.2	66	15.5×35.8	NO
[15]	1.5	66.67	60.8×2.3	NO
[16]	1.96	68.4	34.04×20.44	NO
[17]	2.1	88.5	125.25×24.60	NO
This work	2.40	29.2	25.63×19.70	YES

f_0: center frequency, FBW: fractional bandwidth.

5. SECOND STATE OF THE PROPOSED FILTER

The proposed filter has two filtering characters with the left-most coupled-line connection or disconnection. When being connected, the filter is a band-stop filter (which is analyzed above), and when being disconnected, it is a full resistance filter.

A full resistance filter can be obtained by welding a resistor with a resistance value of 3000 Ω between the left-most coupled-lines. The layout and physical diagram of the filter are shown in Fig. 9.

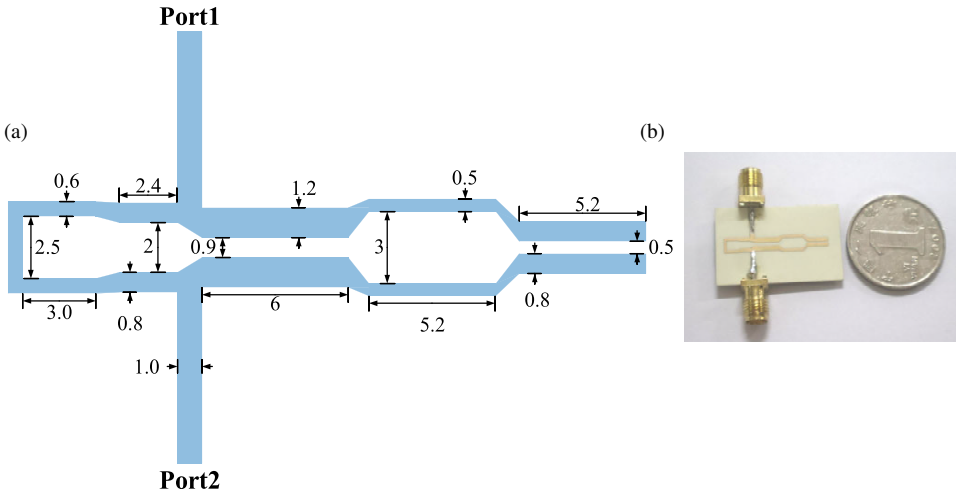

FIGURE 7. The (a) layout and (b) photograph of the fabricated band-stop filter (Unit: mm).

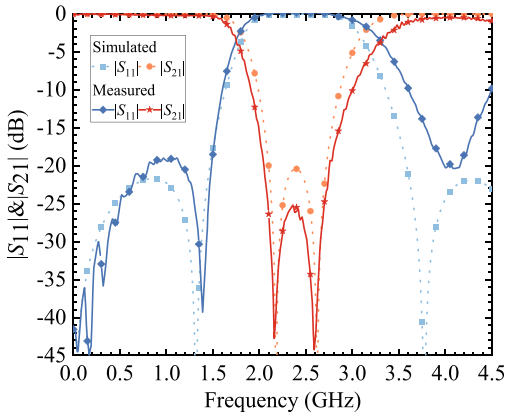

FIGURE 8. Simulated and measured results of the wideband BSF.

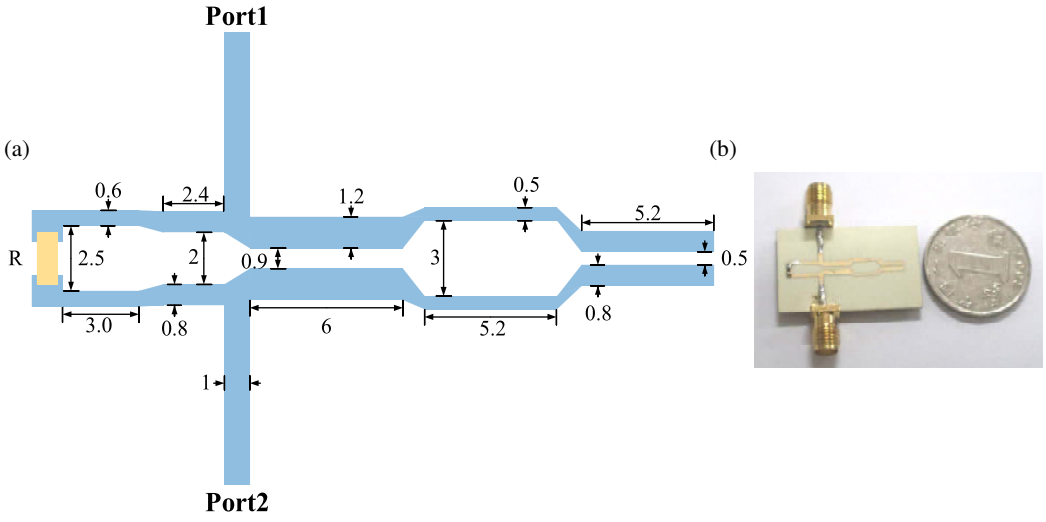

FIGURE 9. The (a) layout and (b) photograph of the total resistance filter (Unit: mm).

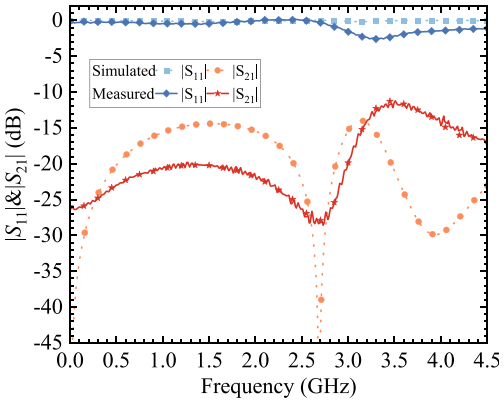

FIGURE 10. Simulated and measured results of the full resistance filter.

Figure 10 shows the simulation and measurement results of the total resistance filter. The insertion loss of the filter is less than 10-dB, and it features a minimum return loss of 3-dB within the frequency range of 0 to 4.5 GHz.

6. CONCLUSION

A new five short coupled-lines band-stop filter circuit structure is proposed. By changing the connection mode of the left-most coupled-line, the band-stop filter can be switched into a full resistance filter. A small size band-stop filter and a full resistance filter are designed. The design theory and circuit configuration are provided, and the full wave simulation and measurement of the two filters are carried out to verify the design method. Also, the circuit size is compact. These filters can be applied to wireless communication system.

ACKNOWLEDGEMENT

This work was supported by the National Natural Science Foundation of China (62201065).

APPENDIX A.

The specific expressions of A, B, C, D, and E are as follows.

$$
\begin{aligned}
A &= -Z_{e2}^2\left(Z_{e3}^2Z_{e4}+Z_{e3}^2Z_{e5}+Z_{e3}Z_{e4}^2\right)\left(Z_{o2}^2Z_{o4}^2+Z_{o1}Z_{o2}Z_{o4}^2+Z_{o1}\left(Z_{o3}^2Z_{o4}+Z_{o3}^2Z_{o5}+Z_{o3}Z_{o4}^2\right)\right)\\
&\quad +Z_{e2}^2Z_{e4}^2\left(Z_{o3}^2Z_{o4}+Z_{o3}^2Z_{o5}+Z_{o3}Z_{o4}^2\right)\left(Z_{o2}^2+Z_{o1}Z_{o2}\right)\\
B &= Z_{e2}^2\left(Z_{e3}^2Z_{e4}+Z_{e3}^2Z_{e5}+Z_{e3}Z_{e4}^2\right)\left(\left(Z_{o2}^2+Z_{o1}Z_{o2}\right)\left(Z_{o3}Z_{o4}+Z_{o3}Z_{o5}+Z_{o4}Z_{o5}\right)+Z_{o1}Z_{o3}Z_{o4}Z_{o5}\right.\\
&\quad \left.+Z_{o2}\left(Z_{o3}^2Z_{o4}+Z_{o3}^2Z_{o5}+Z_{o3}Z_{o4}^2\right)\right)+\left(Z_{e2}^2Z_{e3}Z_{e4}Z_{e5}-Z_{e1}Z_{e2}Z_{e3}^2Z_{e4}-Z_{e1}Z_{e2}Z_{e3}^2Z_{e5}-Z_{e1}Z_{e2}Z_{e3}Z_{e4}^2\right)\\
&\quad \left(Z_{o2}^2Z_{o4}^2+Z_{o1}Z_{o2}Z_{o4}^2+Z_{o1}\left(Z_{o3}^2Z_{o4}+Z_{o3}^2Z_{o5}+Z_{o3}Z_{o4}^2\right)\right)-Z_{e2}^2Z_{e4}^2Z_{o3}Z_{o4}Z_{o5}\left(Z_{o2}^2+Z_{o1}Z_{o2}\right)\\
&\quad -\left(Z_{e2}^2Z_{e3}Z_{e4}+Z_{e2}^2Z_{e3}Z_{e5}+Z_{e2}^2Z_{e4}Z_{e5}+Z_{e1}Z_{e2}Z_{e4}^2+\left(Z_{e1}+Z_{e2}\right)\left(Z_{e3}^2Z_{e4}+Z_{e3}^2Z_{e5}+Z_{e3}Z_{e4}^2\right)\right)\\
&\quad \left(Z_{o3}^2Z_{o4}+Z_{o3}^2Z_{o5}+Z_{o3}Z_{o4}^2\right)\left(Z_{o2}^2+Z_{o1}Z_{o2}\right)\\
C &= -Z_{e2}^2Z_{o2}Z_{o3}Z_{o4}Z_{o5}\left(Z_{e3}^2Z_{e4}+Z_{e3}^2Z_{e5}+Z_{e3}Z_{e4}^2\right)-Z_{e1}Z_{e2}Z_{e3}Z_{e4}Z_{e5}\left(Z_{o2}^2Z_{o4}^2+Z_{o1}Z_{o2}Z_{o4}^2\right.\\
&\quad \left.+Z_{o1}\left(Z_{o3}^2Z_{o4}+Z_{o3}^2Z_{o5}+Z_{o3}Z_{o4}^2\right)\right)-\left(Z_{e2}^2Z_{e3}Z_{e4}Z_{e5}-Z_{e1}Z_{e2}Z_{e3}^2Z_{e4}-Z_{e1}Z_{e2}Z_{e3}^2Z_{e5}-Z_{e1}Z_{e2}Z_{e3}Z_{e4}^2\right)\\
&\quad \left(\left(Z_{o2}^2+Z_{o1}Z_{o2}\right)\left(Z_{o3}Z_{o4}+Z_{o3}Z_{o5}+Z_{o4}Z_{o5}\right)+Z_{o1}Z_{o3}Z_{o4}Z_{o5}+Z_{o2}\left(Z_{o3}^2Z_{o4}+Z_{o3}^2Z_{o5}+Z_{o3}Z_{o4}^2\right)\right)\\
&\quad +Z_{o3}Z_{o4}Z_{o5}\left(Z_{e2}^2Z_{e3}Z_{e4}+Z_{e2}^2Z_{e3}Z_{e5}+Z_{e2}^2Z_{e4}Z_{e5}+Z_{e1}Z_{e2}Z_{e4}^2+\left(Z_{e1}+Z_{e2}\right)\left(Z_{e3}^2Z_{e4}+Z_{e3}^2Z_{e5}+Z_{e3}Z_{e4}^2\right)\right)\\
&\quad \left(Z_{o2}^2+Z_{o1}Z_{o2}\right)+\left(Z_{e1}Z_{e2}Z_{e3}Z_{e4}+Z_{e1}Z_{e2}Z_{e3}Z_{e5}+Z_{e1}Z_{e2}Z_{e4}Z_{e5}-Z_{e1}Z_{e3}Z_{e4}Z_{e5}-Z_{e2}Z_{e3}Z_{e4}Z_{e5}\right)\\
&\quad \left(Z_{o3}^2Z_{o4}+Z_{o3}^2Z_{o5}+Z_{o3}Z_{o4}^2\right)\left(Z_{o2}^2+Z_{o1}Z_{o2}\right)\\
D &= Z_{o2}Z_{o3}Z_{o4}Z_{o5}\left(Z_{e2}^2Z_{e3}Z_{e4}Z_{e5}-Z_{e1}Z_{e2}Z_{e3}^2Z_{e4}-Z_{e1}Z_{e2}Z_{e3}^2Z_{e5}-Z_{e1}Z_{e2}Z_{e3}Z_{e4}^2\right)\\
&\quad +Z_{e1}Z_{e2}Z_{e3}Z_{e4}Z_{e5}\left(\left(Z_{o2}^2+Z_{o1}Z_{o2}\right)\left(Z_{o3}Z_{o4}+Z_{o3}Z_{o5}+Z_{o4}Z_{o5}\right)+Z_{o1}Z_{o3}Z_{o4}Z_{o5}\right.\\
&\quad \left.+Z_{o2}\left(Z_{o3}^2Z_{o4}+Z_{o3}^2Z_{o5}+Z_{o3}Z_{o4}^2\right)\right)-Z_{o3}Z_{o4}Z_{o5}\left(Z_{e1}Z_{e2}Z_{e3}Z_{e4}+Z_{e1}Z_{e2}Z_{e3}Z_{e5}\right.\\
&\quad \left.+Z_{e1}Z_{e2}Z_{e4}Z_{e5}-Z_{e1}Z_{e3}Z_{e4}Z_{e5}-Z_{e2}Z_{e3}Z_{e4}Z_{e5}\right)\left(Z_{o2}^2+Z_{o1}Z_{o2}\right)\\
E &= -Z_{e1}Z_{e2}Z_{e3}Z_{e4}Z_{e5}Z_{o2}Z_{o3}Z_{o4}Z_{o5}
\end{aligned}
$$

REFERENCES

[1] Wu, D.-S., Y. C. Li, and B.-J. Hu, "LTCC wideband bandstop filter with controllable bandwidth using internal coupling," in *2019 International Conference on Microwave and Millimeter Wave Technology (ICMMT)*, 1–3, Guangzhou, China, 2019.

[2] Feng, W., W. Che, S. Shi, and J. Zhou, "Compact dual-wideband bandstop filter based on transversal signal-interference concept," in *2012 Asia Pacific Microwave Conference Proceedings*, 505–507, Kaohsiung, Taiwan, 2012.

[3] Gómez-García, R., J.-M. Muñoz-Ferreras, and D. Psychogiou, "Adaptive multi-band negative-group-delay RF circuits with low reflection," *IEEE Transactions on Circuits and Systems I: Regular Papers*, Vol. 68, No. 5, 2196–2209, 2021.

[4] Zhu, L., S. Sun, and R. Li, *Microwave Bandpass Filters for Wideband Communications*, John Wiley & Sons, Hoboken, New Jersey, 2012.

[5] Zuo, X. and J. Yu, "Miniaturized planar coupled-line bandstop filter with improved and extended pass-band performances," *Microwave and Optical Technology Letters*, Vol. 59, No. 9, 2260–2262, 2017.

[6] Kumar, K. V. P. and S. S. Karthikeyan, "A compact and high performance band-stop filter using open complementary split ring resonator," in *2013 National Conference on Communications (NCC)*, 1–5, New Delhi, India, 2013.

[7] Jones, T. R. and M. Daneshmand, "Miniaturized reconfigurable dual-band bandstop filter with independent stopband control using folded ridged quarter-mode substrate integrated waveguide," in *2019 IEEE MTT-S International Microwave Symposium (IMS)*, 102–105, Boston, MA, USA, 2019.

[8] Sanchez-Soriano, M. A., G. Torregrosa-Penalva, and E. Bronchalo, "Compact wideband bandstop filter with four transmission zeros," *IEEE Microwave and Wireless Components Letters*, Vol. 20, No. 6, 313–315, 2010.

[9] Zhang, C., J.-P. Geng, R.-H. Jin, X.-L. Liang, and L. Liu, "Dual-wideband bandstop filter using stepped impedance coupled-lines," *Microwave and Optical Technology Letters*, Vol. 57, No. 10, 2304–2306, 2015.

[10] Chen, F.-C., R.-S. Li, and J.-P. Chen, "A tunable dual-band bandpass-to-bandstop filter using pin diodes and varactors," *IEEE Access*, Vol. 6, 46 058–46 065, 2018.

[11] Shareef, A. M. and K. H. Sayidmarie, "Compact reconfigurable band-reject/all-pass microstrip filter using U-shaped slot," in *2022 4th International Conference on Advanced Science and Engineering (ICOASE)*, 49–54, Zakho, Iraq, 2022.

[12] Simpson, D. J., R. Gómez-García, and D. Psychogiou, "Tunable multiband bandpass-to-bandstop RF filters," in *2018 IEEE/MTT-S International Microwave Symposium — IMS*, 1363–1366, Philadelphia, PA, USA, 2018.

[13] Ram, G. C., P. Sambaiah, S. Yuvaraj, and M. V. Kartikeyan, "Tunable bandstop filter using graphene in terahertz frequency band," *AEU — International Journal of Electronics and Communications*, Vol. 144, 154047, 2022.

[14] Rajput, A., P. K. Gupta, M. Chauhan, and B. Mukherjee, "Wideband bandstop filter design with high impedance folded stubs," in *2022 IEEE Wireless Antenna and Microwave Symposium (WAMS)*, 1–5, Rourkela, India, 2022.

[15] Mandal, M. K., K. Divyabramham, and S. Sanyal, "Compact, wideband bandstop filters with sharp rejection characteristic," *IEEE Microwave and Wireless Components Letters*, Vol. 18, No. 10, 665–667, 2008.

[16] Tang, C.-W. and C.-H. Yang, "New method for the microstrip bandstop filter with a wide stopband and an extremely high attenuation," *IEEE Transactions on Circuits and Systems II: Express Briefs*, Vol. 69, No. 11, 4318–4322, 2022.

[17] He, M., X. Zuo, H. Mei, and Y. Li, "A planar sharp-attenuation ultra-wideband bandstop filter with a three section coupled-line stub," *Progress In Electromagnetics Research C*, Vol. 146, 195–199, 2024.